www.railwaygazette.com MAY 2022

Railway Gazette
INTERNATIONAL

Making tracks to Münster

MAINTENANCE
Rethinking rail asset management strategies in Northern Ireland
Page 20

FAR EAST
Express metro lines serve China's expanding conurbations
Page 46

IN FOCUS
French regulator addresses barriers to market entry
Page 54

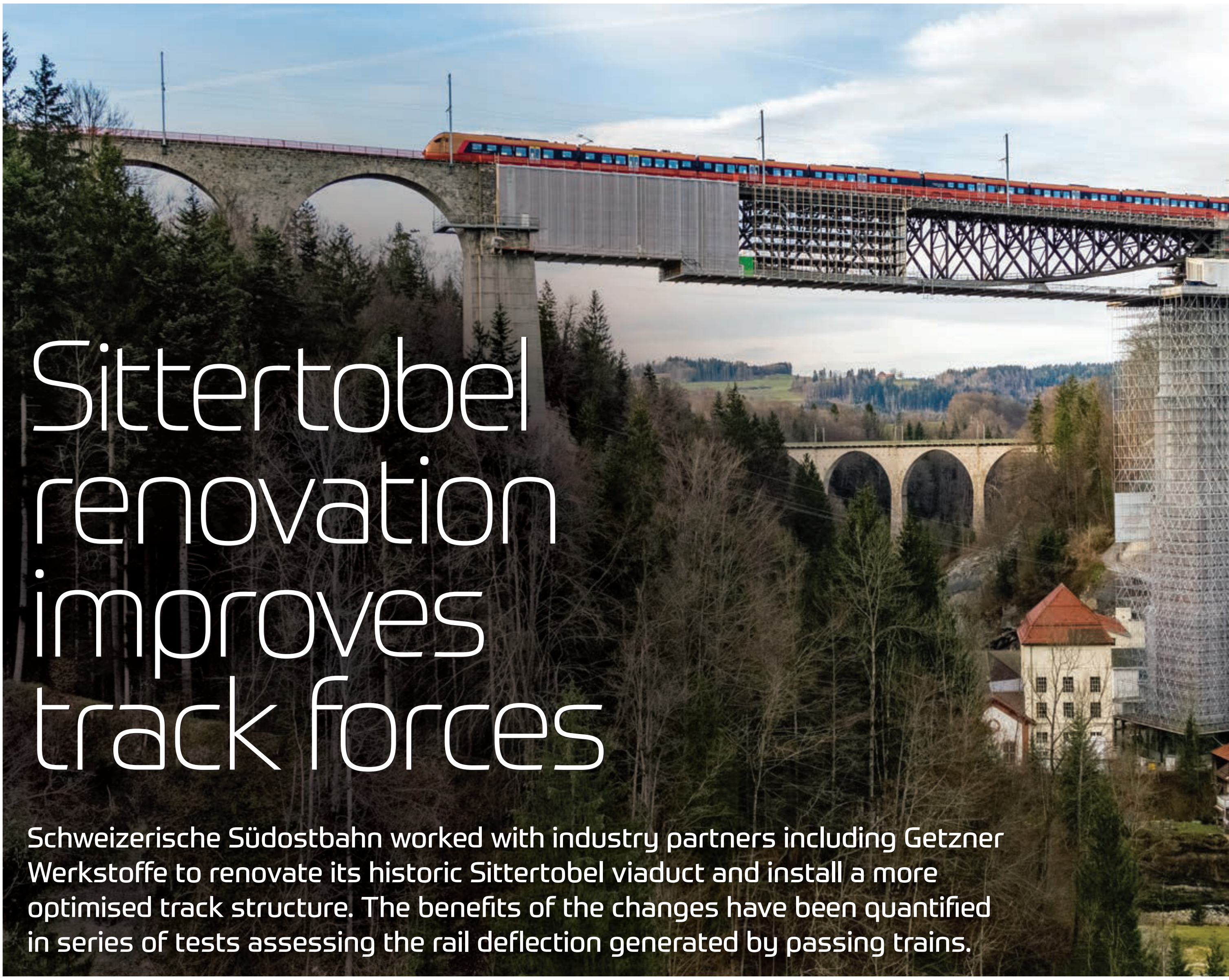

Sittertobel renovation improves track forces

Schweizerische Südostbahn worked with industry partners including Getzner Werkstoffe to renovate its historic Sittertobel viaduct and install a more optimised track structure. The benefits of the changes have been quantified in series of tests assessing the rail deflection generated by passing trains.

Dipl-Ing Martin Quirchmair
Corporate Development,
Getzner Werkstoffe
Dipl-Ing Stefan Werner
KPZ Fahrbahn AG
Dipl-Ing Beat Burgherr
SOB Infrastruktur
Dr Harald Loy
Getzner Werkstoffe/ITS University
Innsbruck

Located on the approach to St Gallen, the Sittertobel viaduct on the Schweizerische Südostbahn is one of the most imposing railway structures in the Alps. Completed in 1910, the 99 m high viaduct is the tallest railway bridge in Switzerland. The 365 m long structure comprises two approach viaducts and a 120 m long steel truss girder main span across the Sitter River; this so-called ‘fish belly’ is up to 12 m in height and weighs approximately 920 tonnes.

Having passed its centenary, the structure has been subject to close attention. Routine inspections in recent years revealed the natural effects of wear and tear on both the approach viaducts and the main span. Because of the strategic importance of the viaduct to the SOB network, as well as its cultural and heritage significance, the railway decided to undertake a comprehensive renewal programme with the aim of equipping it to last a further 50 years without major intervention or replacement[1].

Feasibility studies confirmed that the repairs were viable, both technically and commercially. Work started in 2019 and was concluded in 2021. In addition to the restoration of the viaduct itself, the entire track superstructure was renewed, with a redesigned transition zone between the open deck and the ballasted track elements, and the relocation of the rail expansion joint.

1910
Year the Sittertobel viaduct was completed

Prior to the reconstruction, the approach viaducts were laid with a ballast trough and wooden sleepers. The southern (Herisau) end of the bridge has more approach spans than the northern (St Gallen) end, and also includes a 350 m radius curve. Reflecting the load-bearing capacity of the steel truss girder, a considerably lighter open deck was used for the centre span. Specialist bridge sleepers were mounted on rubber pads, which provided additional elasticity to the track.

Expansion joints were fitted to the rails, with their centres approximately 4 m from the Herisau end of the fish belly. However, pronounced void

The Sittertobel viaduct is 365 m long with a maximum height of 99 m, making it the tallest railway structure in Switzerland.

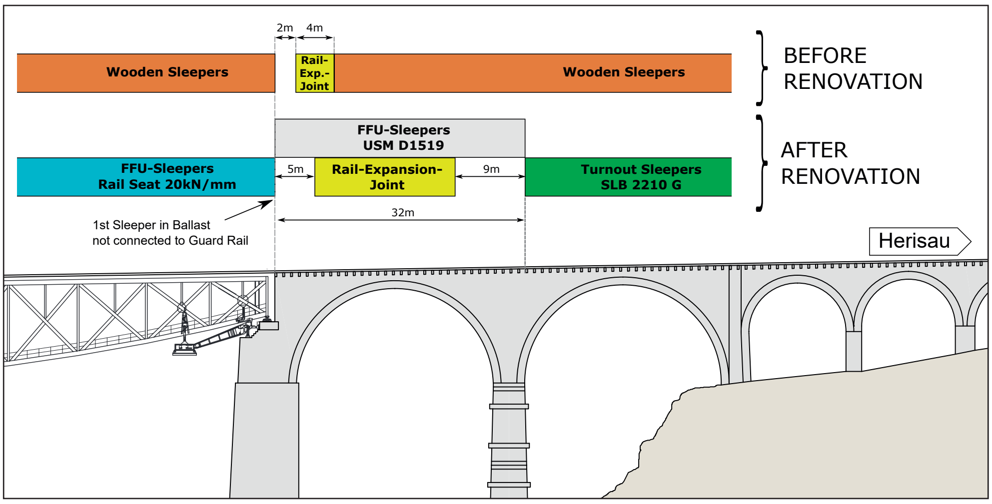

Fig 1. Track and superstructure configuration before and after the renovation work.

formation was apparent around the joint, with signs of wear and ballast degradation. This meant that maintenance intervals on this part of the viaduct were shorter than elsewhere, with increased costs. Addressing the varying track stiffness around the joint was therefore a key focus for the bridge renovation project.

On long bridges, the rail expansion joints are typically located close to the expansion joints for the structure itself. They are thus able to absorb longitudinal track movements as the structure expands and contracts and prevent excessive rail stress resulting from thermal length variations and dynamic loads.

In Switzerland, the requirements for track over bridges are set out in SBB's technical standard I-22068. This also describes the use of expansion compensating devices according to the length and type of bridge[2]. The principle behind the rail expansion joint is shown in Fig 2. In the centre of the joint, the switch and stock rails are pressed against each other by braces. The rail ends can slide against each other, compensating for any movement in the bridge. Modern rail expansion joints can typically expand by 1 200 mm or more.

However, the rail expansion joint causes a local change in the structure's characteristics; this may result in load peaks under dynamic loading conditions. It was no surprise that increased signs of wear, such as ballast destruction and voids, were appearing in the area around the expansion joint.

Redesigned superstructure

Redesign of the superstructure was managed by Kompetenzzentrum Fahrbahn AG. Because of difficulty in replacing the sleepers on the fish belly, KPZ decided early on to dispense with wooden sleepers and use weatherproof fibre-reinforced foamed urethane sleepers. Elsewhere, the standard ballasted track has been relaid using conventional concrete sleepers rather than timber. In the area around the transitions between the bridge track and the ballasted track, it was decided to deploy heavier concrete turnout sleepers.

The problem areas were physically separated to alleviate the problems that had been caused by the combination of the transition zones and the rail expansion joint. The centre of the rail expansion joint was moved outwards to 14 m from the end of the fish belly. Elastic rail seats from Delkor were installed on the main span in order to adapt the stiffness of the open deck bridge track to that of the ballasted sections (Fig 1).

Track elasticity

The adjustment in stiffness at the transitions between the fish belly and the approach viaducts was carried out with the help of FEM modelling. The structural design concept had been developed by KPZ, and from there the elasticity of the track could be optimised.

Based on calculations carried out using various product combinations, the configuration shown in Fig 1 was

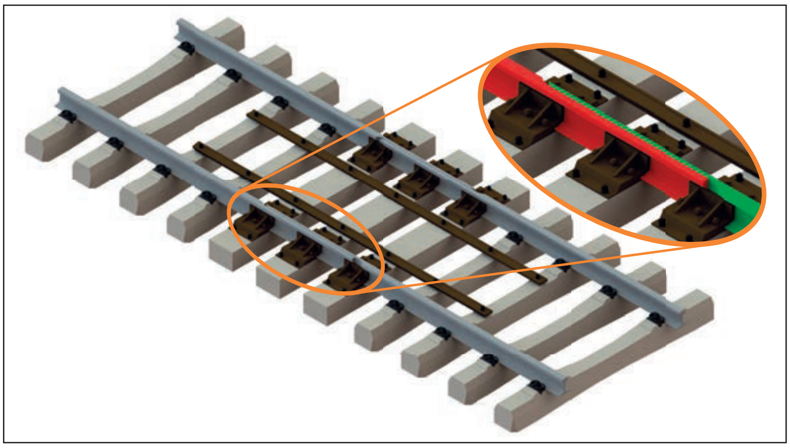

Fig 2. The basic arrangement of the rail expansion joint, where the switch rails (green) and stock rails (red) are pressed against each other by rail braces and can absorb longitudinal movements.

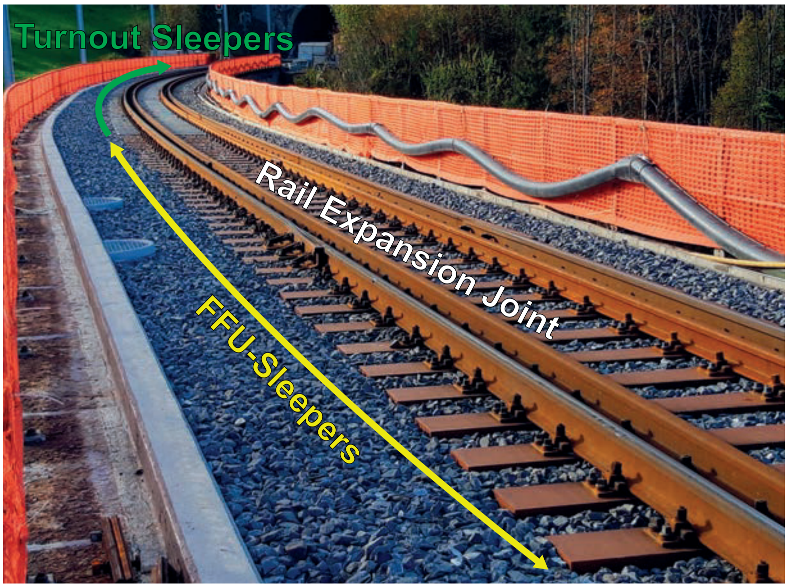

Fig 3. A view of the approach viaduct following restoration. The guard rails extend over the entire length of the structure.

30 h

Total traffic observation period at the measurement zone

determined to be the most appropriate. A stiffness value of 20 kN/mm was set for the rail seats on the open deck. A D1519 under-ballast mat with a bedding stiffness of 0·15 N/mm^3 was laid under the ballasted track on the approach spans in the vicinity of the rail expansion joint, which was also supported on FFU sleepers. The turnout sleepers which support the connection to the standard track superstructure were equipped with elastoplastic SLB 2210 G under-sleeper pads. These are designed to preserve the track alignment and protect the ballast. Fig 3 shows the restored superstructure of the approach viaduct from the Herisau end.

Guard rails have also been installed next to the 54E2 running rails; these extend across the entire length of the viaduct and function as a safety measure, preventing a derailed train from reaching the edge of the bridge. From a technical perspective, they are also used to adjust stiffness in the transition zones. However, this approach can sometimes lead to problems in the longer term, as the guard rails can affect the mechanical loading of the superstructure components.

This question therefore had to be addressed when dealing with the transition zone. The stiffening effect of the guard rails on the ballasted track sections generates higher forces, particularly at the connection between the fish belly and the approach spans. This happens because guard rails on the open deck section have almost no impact on track stiffness, which is dominated by the soft rail seats that sit on the rigidly bedded FFU sleepers and almost completely decouple the running rails from the guard rails.

In particular, the first sleeper on the ballasted track is held in position by the fixing of the guard rails on the open deck. This results in less deflection and produces an imperfection in the track. The higher forces at the transition can be seen in the calculated deflection curve (Fig 4). A simple way to mitigate this effect was to remove the connection of the guard rails from the first FFU sleeper on the ballasted track section. Modelling showed that this would result in a significantly more homogeneous deflection in the transition zone, which in turn had a direct impact on the dynamic forces. Fig 4 shows the computational simulation of this change, which could then be incorporated into the planning of the restoration work[3].

Measuring the results

To verify the improvements brought about by the structural restoration, Getzner Werkstoffe performed 'before and after' track geometry measurements in May 2019 and September 2020.

In order to analyse track performance in the transition zone, the Getzner team focused on measuring rail deflection. Four measuring sections marked M1 to M4 were set out as shown in Fig 5.

M1 was located on the main span and captured the deflections on the open deck. Deflection at the rail expansion joint was measured at M2. Because the centre of the rail expansion joint was moved during the restoration, the two locations are marked in Fig 5 as '2019' and '2020'. Sections M3 and M4 were used to determine the deflection of the FFU sleepers and the padded turnout sleepers. These two sections were located at the start of the 350 m radius curve on the Herisau approach.

Vibrations in the structure were measured at M5. In this context, the vibrations were seen purely as a measure of the dynamic load of a passing train. If these could be reduced, the load exerted on the track superstructure and hence on the structure itself, would also be reduced.

Rail deflection at M1, M3 and M4 was measured using the approach shown in Fig 6. On the assumption that the tilting of the rail φ is low and any

Below: Fig 4. The calculated deflection curve at the transition between the fish belly and approach spans. The guard rail is fastened to or loosened from the first sleeper on the ballasted track.

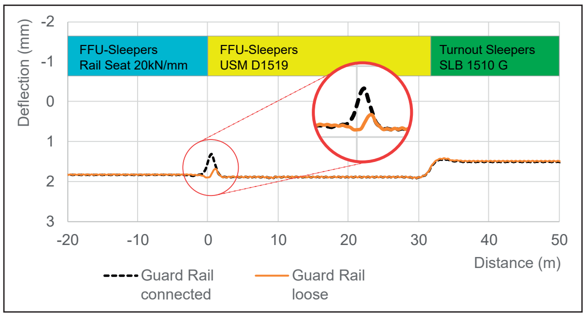

Right: Fig 5. The measuring methodology showing the data collection points in 2019 and 2020 to enable a 'before and after' comparison of the behaviour of the superstructure.

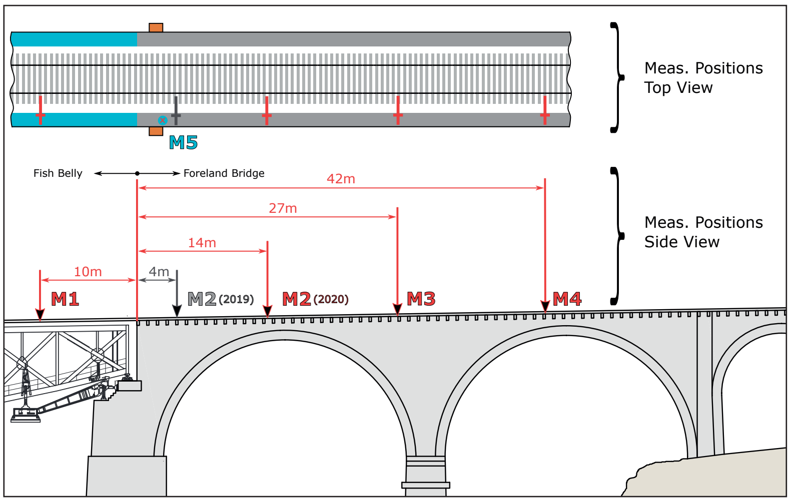

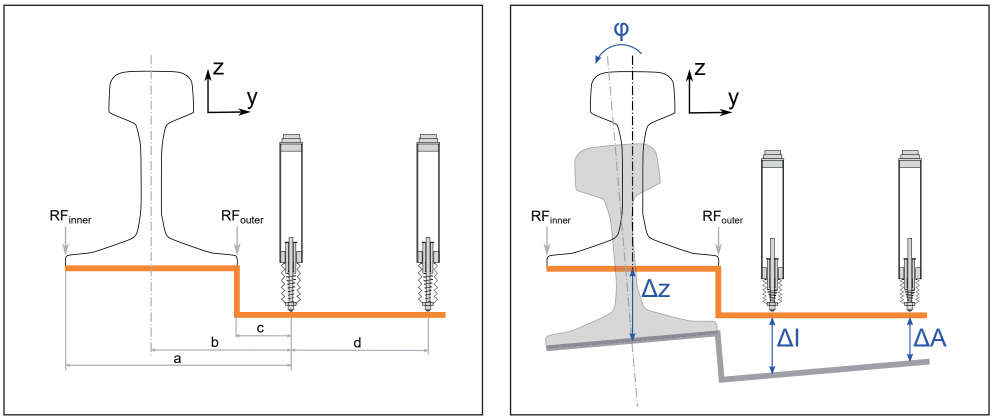

Fig 6. The deflection measurement calculation at points M1, M3 and M4.

Fig 7. The measuring setup in the field before restoration. Points M2, M3 and M4 are deflection measurements. The role of the trigger is to start the measurement automatically.

movement in the y-direction negligible, a geometric relationship enables the deflection Δz at the middle of the rail base to be derived, and from that the deflection at the two rails (RF_{inner} and RF_{outer}).

A maximum error of less than 3% was estimated for the expected deflection figures, and this was deemed to be sufficiently accurate. In the centre of the rail expansion joint (M2), the rail is split between the switch and stock rails. The measurements were taken directly on the rail base, so that the observed deflections could be used in the evaluation without having to be transformed.

The field setup is shown in Fig 7. Vibrations were measured at M5; the acceleration sensor was bonded to the granite structure precisely at the connection between the fish belly and the approach span.

As the measurements could only be taken with people on site at the beginning, it was decided to trigger them automatically, using an acceleration sensor placed on a sleeper on the fish belly. This allowed around 15 h of normal operation to be recorded, for both the before and after campaigns.

Evaluating the outcome

In regular service, three types of passenger trains normally pass over the Sittertobel viaduct: SOB's Stadler Flirt EMUs, Thurbo's GTW EMUs, and SOB's *Voralpenexpress* inter-regional services; these were initially operated by locomotive-hauled push-pull formations, but were replaced from mid-2019 by new Stadler Traverso EMUs.

Because of the restoration work on the track superstructure and the viaduct itself, a speed restriction was in place at the time of the measurements; trains were limited to 50 km/h, rather than the regular line speed of 80 km/h. In measuring sections M1, M3 and M4, the deflection in the middle of the rail foot was calculated. For the rail expansion joint (M2), the deflection in the middle of the rail foot could not be measured or calculated in any meaningful way due to the split in the rails. It was decided to use the outer stock rail for the evaluation, as it would be bearing the greater part of the load at the measurement location.

The maximum rail deflection values under the most heavily loaded axles as measured at M1 to M4 were used to calculate an average value for each train and measuring point. Four passes of each type of train were used for the evaluation, ensuring a representative average. This method enabled a deflection value to be derived from the before and after measurements. The vibrations at M5 were evaluated for the same four passes of each type of train.

Measurement results

All four train types showed results of comparable magnitude in terms of deflection and vibration. As a result, our assessment of the improved track alignment used the average results from all the train passes before and after the restoration. The following discussion looks at an example of a Flirt EMU travelling towards Herisau[4].

Fig 8 shows the deflection curves for both 2019 and 2020. In both cases, M1 on the fish belly measured a uniform deflection with no tilting of the rail. Before restoration, the amount of deflection was primarily dictated by the rubber pads under the bridge sleepers. After reconstruction, the required level of elasticity was provided by the elastic rail seats.

The rail expansion joint was measured at M2. Significant differences were observed after the reconstruction, and the new position of the joint can be seen in the time signal. In 2019, a large deflection was observed during the passage of a train, which is particularly noticeable in the graph of the stock rail (marked 'outer'). This showed significantly more deflection than the switch rail ('inner'). The deflection of more than 4 mm was also significantly greater than the rest of the track. After

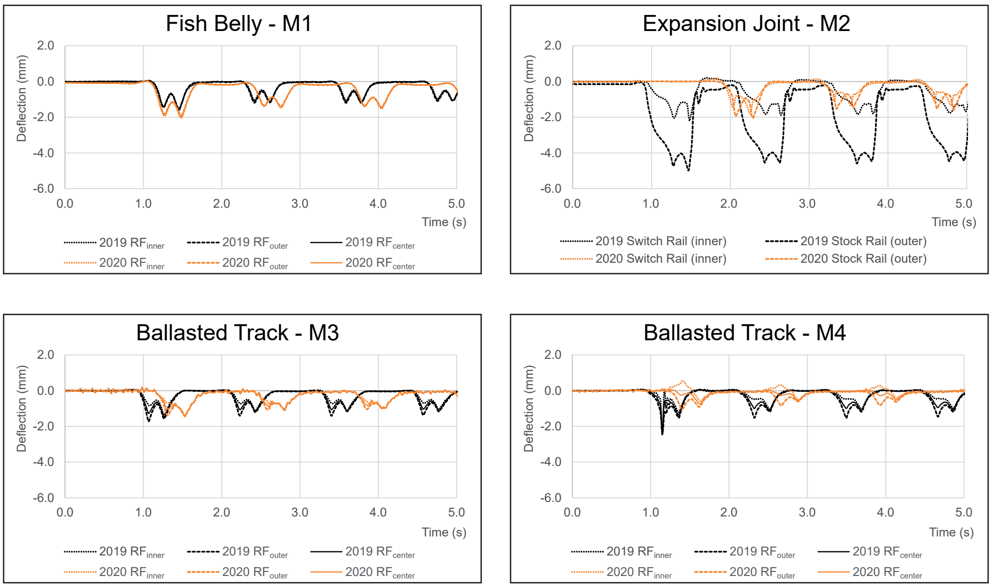

Fig 8. An overview of the results at positions M1 to M4 as a Flirt EMU passes over the viaduct. RF_{inner}, RF_{outer} and RF_{center} represent the positions on the rail base.

reconstruction, the amount of deflection for the switch and stock rails was more or less identical. The time offset of the two measuring signals shows how the wheel load transfers from switch rail to stock rail (Fig 9). The rail expansion joint now has a deflection of about 2 mm and is very well adapted to the standard track.

Slightly less rail deflection was evident at M3 and M4. What was apparent was that the rail tilted noticeably, particularly at M4. This was located well into the curve, where the outer rail was superelevated. As the trains were restricted to 50 km/h at the time of the measurement, we believe that the train slipped towards the centre as it took the curve, pressing on the head of the inner rail. An increased rotation of the rail was therefore to be expected, with movement in the y direction. As such, it is possible that slightly different deflections would have been observed had the trains been running at normal speeds.

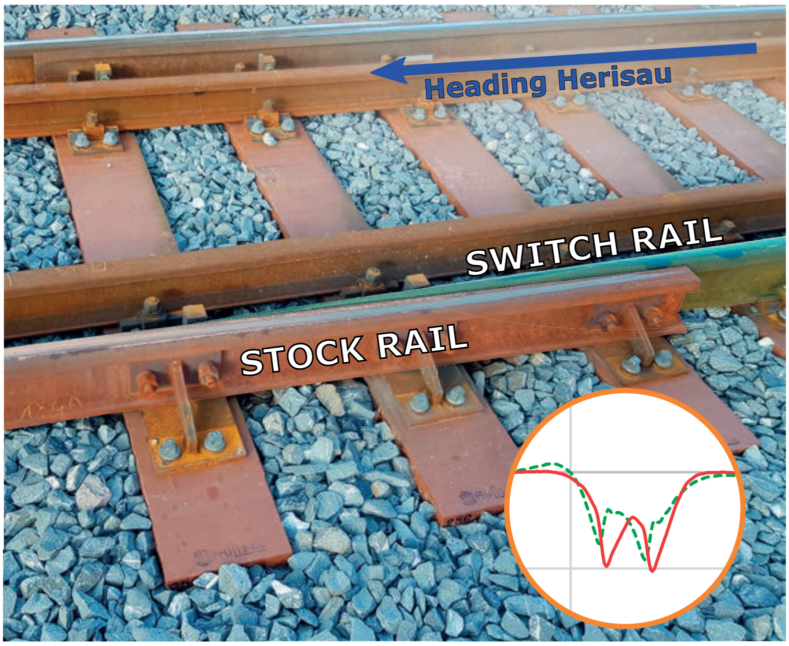

Fig 9. Following restoration, the transfer of the wheel load from the switch rail to the stock rail was reflected in the measurement data.

Homogenous behaviour

After averaging out all the evaluated train passes, it is clear that the new superstructure design exhibits a much more homogeneous deflection curve (Fig 10). There has been a significant improvement to the transition zone, including the rail expansion joint.

The vibration measurements at M5 were used to assess the homogeneity of the transition with regard to the transfer of kinetic energy to the structure as a train passes. This is a measure of the uniformity of the track bed where the superstructure changes, and the force peaks arising as a result. Here the priority was to assess the measured spectrum as a whole, as impacts caused by faults in the superstructure generally lead to wide-band excitation.

The before/after comparison in Fig 11 shows the measured third-octave spectrum. The scatter band is defined by the minimum and maximum values of all the passing trains evaluated. At first glance, it seems surprising that there was no visible improvement in the 31·5 Hz to 63 Hz range. The most probable reason for this is the choice of elastic components, which were dimensioned with a focus on optimising the transition. If one considers the natural frequencies of the fish belly with elastic rail fastening systems and those of the ballasted track with a rigid under-ballast mat, the result lies in the 30 Hz to 40 Hz range.

Using a simple mass-spring model, an improvement starting at approximately 60 Hz would be possible, although, to make a fair comparison, the natural frequencies prior to the restoration would also have to be considered. However, in this situation a rough estimate is sufficient, as the change from a lattice girder structure to a stone arch bridge makes the conditions in the transition zone increasingly undefined, giving us less confidence in the analytical result.

Nevertheless, the measurement as a whole shows a reduction in the vibrations transmitted into the viaduct of around 5 dB, with the levels of the estimated frequency bands deemed critical in terms of resonance staying the same. The vibration measurements support the results showing a more homogeneous transition as observed in the deflection measurements.

5
dB

Reduction in vibration levels after the renovation work

References

1. Wagner, R., *Instandsetzung des Sitterviadukts*; 19. Symposium Brückenbau in Leipzig; Ausgabe 1/2 2019.
2. SBB; standard I-22068: *Anforderungen der Fahrbahn an Brücken und oberbautechnische Massnahmen im Einflussbereich der Brücken*, 2015.
3. SOB Plan 1392.3302, 2018.
4. Getzner Werkstoffe; Report 2020-086-REV3: *Gleismessungen am Sitterviadukt im Gleisnetz der Schweizerischen Südostbahn AG*; Internal Report, Bürs, 2020.

Below left: Fig 10. Average rail deflection before (2019) and after (2020) restoration.

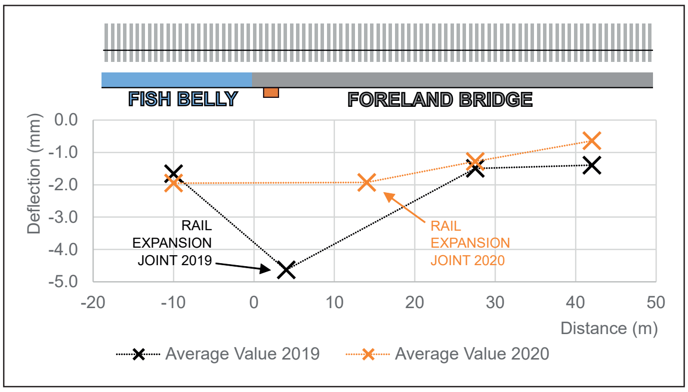

Below: Fig 11. Vibration measurement results at the transition between the fish belly and the approach viaduct.